27. Gnekow AK, Kortmann RD, Pietsch T, Emser A. Low grade chiasmatic-hypothalamic glioma-carboplatin and vincristin chemotherapy effectively defers radiotherapy within a comprehensive treatment strategy—report from the multicenter treatment study for children and adolescents with a low grade glioma—HIT-LGG 1996—of the Society of Pediatric Oncology and Hematology (GPOH). *Klin Padiatr.* 2004;216:331–342.

28. Marcus KJ, Goumnerova L, Billett AL, et al. Stereotactic radiotherapy for localized low-grade gliomas in children: final results of a prospective trial. *Int J Radiat Oncol Biol Phys.* 2005;61:374–379.

29. Parsa CF, Hoyt CS, Lesser RL, et al. Spontaneous regression of optic gliomas: thirteen cases documented by serial neuroimaging. *Arch Ophthalmol.* 2001;119:516–529.

30. Palma L, Celli P, Mariottini A. Long-term follow-up of childhood cerebellar astrocytomas after incomplete resection with particular reference to arrested growth or spontaneous tumour regression. *Acta Neurochir (Wien).* 2004;146:581–588.

EXPRESSIVE AND RECEPTIVE LANGUAGE AREAS DETERMINED BY A NON-INVASIVE RELIABLE METHOD USING FUNCTIONAL MAGNETIC RESONANCE IMAGING AND MAGNETOENCEPHALOGRAPHY

Kyousuke Kamada, M.D., Ph.D.
Department of Neurosurgery, The University of Tokyo, Tokyo, Japan

Yutaka Sawamura, M.D., Ph.D.
Department of Neurosurgery, Hokkaido University, Sapporo, Japan

Fumiya Takeuchi, Ph.D.
Research Institute for Electric Science, Hokkaido University, Sapporo, Japan

Shinya Kuriki, Ph.D.
Research Institute for Electronic Science, Hokkaido University, Sapporo, Japan

Kensuke Kawai, M.D., Ph.D.
Department of Neurosurgery, The University of Tokyo, Tokyo, Japan

Akio Morita, M.D., Ph.D.
Department of Neurosurgery, The University of Tokyo, Tokyo, Japan

Tomoki Todo, M.D., Ph.D.
Department of Neurosurgery, The University of Tokyo, Tokyo, Japan

Reprint requests:
Kyousuke Kamada, M.D., Ph.D., and Tomoki Todo, M.D., Ph.D., Department of Neurosurgery, The University of Tokyo, 7-3-1 Hongo, Bunkyo-ku, Tokyo 113-8655 Japan.
Email: kamady-k@umin.ac.jp

Received, March 23, 2006.
Accepted, October 13, 2006.

OBJECTIVE: It is known that functional magnetic resonance imaging (fMRI) and magnetoencephalography (MEG) are sensitive to the frontal and temporal language function, respectively. Therefore, we established combined use of fMRI and MEG to make reliable identification of the global language dominance in pathological brain conditions.

METHODS: We investigated 117 patients with brain lesions whose language dominance was successfully confirmed by the Wada test. All patients were asked to generate verbs related to acoustically presented nouns (verb generation) for fMRI and to read three-letter words for fMRI and MEG.

RESULTS: fMRI typically showed prominent activations in the inferior and middle frontal gyri, whereas calculated dipoles on MEG typically clustered in the superior temporal region and the fusiform gyrus of the dominant hemisphere. A total of 87 patients were further analyzed using useful data from both the combined method and the Wada test. Remarkably, we observed a 100% match of the combined method results with the results of the Wada test, including two patients who showed expressive and receptive language areas dissociated into bilateral hemispheres.

CONCLUSION: The results demonstrate that this non-invasive and repeatable method is not only highly reliable in determining language dominance, but can also locate the expressive and receptive language areas separately. The method may be a potent alternative to invasive procedures of the Wada test and useful in treating patients with brain lesions.

KEY WORDS: Expressive language function, Functional magnetic resonance imaging, Language dominance, Magnetoencephalography, Receptive language function

Neurosurgery 60:296–306, 2007 DOI: 10.1227/01.NEU.0000249262.03451.0E www.neurosurgery-online.com

Brain asymmetries have been of considerable interest in neurology for more than a century. Based on clinicopathological studies, the "classical mode" of language organization consists of a frontal "expressive" area for planning and executing speech and writing, and a temporal "receptive" area for analysis and identification of linguistic sensory stimuli. This basic scheme of language functions has generally been accepted, with the assumption that both expressive and receptive functions dominantly exist in the same hemispheric side.

The Wada test has been considered the most reliable method to determine language dominance. According to one of the largest studies performed to date, 4 and 96% of right-handed subjects with chronic epilepsy have speech dominance in the right and left hemispheres, respectively (3). Furthermore, several studies suggested the possibility of atypical language representation in patients with chronic epilepsy (20–30%) (9, 28). However, the procedure of successive anesthetization of each hemisphere by intracarotid injections of sodium amobarbital requires catheterization and irradiation. Furthermore, the Wada test results can only demonstrate a relative distribution of language functions across the two hemispheres. More detailed information on localization of specified language functions within a hemisphere is important for understanding the language networks, as well as the treatment of brain lesions.

The use of functional magnetic resonance imaging (fMRI) has recently been developed to identify the hemisphere with language dominance. Most language fMRI studies have observed activations in the inferior frontal gyrus (IFG) and middle frontal gyrus (MFG) using tasks such as word generation and categorization (16, 24, 29). Detection of the receptive language area by fMRI has been reported to be more difficult than that of the expressive language function, and the use of listening or sentence comprehension tasks has resulted in visualization of only a few pixels in the temporoparietal region (8, 16, 25, 26). In addition, a fundamental limitation of an fMRI-based brain mapping is the varying degrees of regional hemodynamic responses under pathological brain conditions (7, 10, 15). Therefore, a clinical interpretation of localized activations on fMRI remains complicated and controversial.

Magnetoencephalography (MEG) reflects intracellular electric current flow in the brain and allows accurate localization of the current dipole sources. Dipoles of MEG deflections that peaked at approximately 400 milliseconds after word presentation (late responses) have been observed to localize in the temporoparietal regions. These late responses have been considered to be related to the receptive language function (19, 20). We have also observed dense dipole clusters of the semantic late responses in the superior temporal gyrus (STG), supramarginal gyrus (SmG), and fusiform gyrus (FuG) of the suspected dominant hemisphere (11, 12). Therefore, we sought to use MEG not only as an additional diagnostic tool for identifying the language dominance, but also to localize the receptive language center.

In the present study, we describe a non-invasive method to locate the expressive and receptive language areas by co-utilizing fMRI and MEG. The language dominance determined by our method matched the results from the Wada test with 100% accuracy. The usefulness of the method was well demonstrated, especially in those patients who showed dissociated expressive and receptive language functions. The data show that this method is highly reliable and may be useful in the management of patients with brain lesions as well as in studying normal brain functions.

METHODS

Patients

The functional brain mapping using fMRI (with the verb generation task) and MEG was performed in 117 patients with brain lesions since August 1999 (>7 yr) after this project was approved by the Institutional Committee for Ethics (*Table 1*). fMRI studies with the abstract/concrete (A/C) categorization task were also performed in 106 patients. Ninety-seven patients also underwent the Wada test to confirm the dominant cerebral hemisphere for language functions. Six patients showed negative Wada test results owing to the steal effect of a large arteriovenous malformation (AVM) or an overdose. The final analyses were performed in 87 patients (48 men, 39 women), who underwent Wada test, fMRI, and MEG investigations. The mean age (± standard deviation) was 43.6 ± 14.1 years. The Edinburgh Handedness Inventory was used to estimate the patients' handedness (18). A written informed consent was obtained from the patient or his/her family before participation in the study.

Magnetic Resonance Protocols

Anatomic magnetic resonance imaging (MRI) and fMRI were performed during the same session with a 1.5-T whole-body magnetic resonance scanner with echo-planar capabilities and a standard whole-head transmit-receiver coil (Siemens Vision, Erlangen, Germany). During the procedures, foam cushions were used to immobilize the head.

Language fMRI

The patients were instructed to respond to all language tasks silently. fMRI data was acquired with a T2-weighted echo-planar imaging sequence (echo time, 62 ms; repetition time, 114 ms; flip angle, 90 degrees; slice thickness, 4 mm; slice gap, 2 mm; field of view, 260 mm; matrix, 64 × 128; 14 slices). Each fMRI session consisted of three dummy scan volumes followed by three activation and four baseline (rest) periods. During each period, five echo-planar imaging volumes were collected, yielding a total of 38 imaging volumes and 2 minutes 32 seconds in measurement time for each session. fMRI data of language-related semantic responses were acquired as follows. All subjects were examined with two different lexical semantic language paradigms; verb generation by listening to nouns and A/C categorization by reading words. All words for semantic tasks were selected from common Japanese words listed in the electronic dictionary of the National Institute for Japanese Language.

Verb Generation Task

For the auditory stimuli (duration ranges were between 400 and 600 ms), common concrete nouns spoken by a native Japanese speaker with a flat intonation were recorded and digitized with a sampling rate of 44,000 Hz. A backward playback of the sound files (reference sounds) was used to eliminate the primary auditory activation during the rest periods with the same inter-stimuli intervals (1600–2400 ms) as the active periods. The auditory stimuli were delivered binaurally via two 5-m-long plastic tubes terminating at a headphone. The sound intensity was approximately 95 dB sound pressure level at the subject's ear. Subjects were instructed to silently generate a verb related to each presented noun during the active periods and passively listen to the reference sounds during the rest periods.

A/C Categorization Task

Visual stimuli were presented on a liquid crystal display monitor with a mirror above the head coil allowing the patients to see the stimuli. Words consisting of three *Kana* letters (Japanese phonetic symbols) were presented in a 300-millisecond exposure time with interstimuli intervals ranging from 2800 to 3200 milliseconds. Patients were instructed to categorize the presented word silently into "abstract" or "concrete" based on the

TABLE 1. Summary of patients' brain lesions types[a]

	Glioma	Chronic Epilepsy	AVM	Meningioma	Cavernous malformation	Cerebral ischemia	Total
fMRI with VG + MEG	44	39	18	6	4	6	117
fMRI with A/C	41	34	15	6	4	6	106
Amytal test	42	29	16	6	4	0	97
Final analyses	39	26	12	6	4	0	87

[a] AVM, arteriovenous malformation; fMRI, functional magnetic resonance imaging; VG, verb generation task; MEG, magnetoencephalography; A/C, abstract/concrete categorization task.

nature of the word. During interval periods, patients passively viewed random dots of destructured *Kana* letters that were controlled to have the same luminance as the stimuli to eliminate primary visual responses.

Before scanning, all patients had a brief practice time, and the fMRI examinations were repeated for each task to confirm the reproducibility. After data acquisition, a motion detection program (MEDx; Medical Numerics, Sterling, VA) discarded fMRI sessions containing motion artifacts exceeding 25% of the pixel size. A Gaussian spatial filter (6 mm in half width) was applied, and functional activation maps were calculated by estimating the Z-scores between the rest and activation periods using Dr. View (Asahi Kasei, Tokyo, Japan). Pixels with Z-scores higher than 2.2 ($P < 0.05$) were considered to indicate real activation and were used for mapping. Image distortion of fMRI was corrected by maximizing the mutual information of the fMRI data sets and three-dimensional T1-weighted MRI (3D-MRI) scans of the patient's brain (morphing compensation). The result from each fMRI session was co-registered with the 3D-MRI by the Affine transformation (5). After total number of the activated pixels in the IFG and MEG were automatically counted, a patient was considered to have unilateral language dominance when hemispheric pixels of one hemisphere counted less than 70% of the other hemisphere. Otherwise, the language dominance was considered bilateral.

Language MEG

The MEG signals were recorded with a 204-channel biomagnetometer (VectorView; Neuromag, Helsinki, Finland) in a magnetically shielded room. To confirm the reproducibility, we acquired two data sets for each task by repeating the MEG recording on two different days. One hundred fifty nouns consisting of three *Kana* letters were visually presented with a 300-millisecond exposure time with interstimuli intervals ranging from 2800 to 3200 milliseconds. Patients were instructed to judge whether or not the presented word was "abstract" or "concrete" based on the nature of the word and to push a button with the index or middle finger (*Kana* reading task). Each epoch consisted of a 500-millisecond prestimulus baseline and a stimulus followed by a 1500-millisecond analysis period. Epochs with a reaction time exceeding 1200 milliseconds and MEG examinations with a successful task performance less than 70% were discarded.

One hundred fifty epochs of the magnetic signals were averaged and digitally filtered between 0.1 to 30 Hz. Significant MEG deflections were visually identified based on the square root mean fields of more than 10 sensors in the frontotemporal (FT) or temporo-occipital (TO) regions. Locations and dipole moments of equivalent current dipoles were calculated every 2 milliseconds from 250 to 600 milliseconds after the stimulus onsets using the single equivalent dipole and sphere head models. Only those dipoles of which the measured and the calculated field distributions showed a correlation value of more than 0.85 and confidence volumes less than 1000 mm^3 were used. To confirm the calculated results, the same MEG time sections were analyzed using a current density map (low-resolution tomography; LORETA, Curry, Neuroscan, and Compumedics USA, El Paso, TX). The coordinates of the MEG system were transformed into anatomic 3D-MRI scans by identifying external anatomic fiduciary markers (nasion, left/right preauricular points), and estimated dipoles were superimposed onto the 3D-MRI scans.

Dipoles located in the temporal region, including the STG, MTG, SmG, and FuG, were manually counted. A patient was considered to have unilateral language dominance when hemispheric dipoles of one hemisphere counted less than 70% of the other hemisphere. Otherwise, the language dominance was considered bilateral.

Determination of Language Dominance using fMRI and MEG

On the basis of the results of language fMRI and MEG, we determined language dominance for each patient. When the semantic activation in one side of the IFG and MFG was wider than that of the other side during the language fMRI tasks, a patient was considered to have unilateral dominance for the expressive language function. When one side of the temporal region included more MEG dipoles than the other during the language MEG task, we determined that a patient had laterality of the receptive language function.

The Wada Test

All patients received injections of amobarbital (100 mg in a 10% solution, Amytal; Eli Lilly and Co., Indianapolis, IN) through a catheter placed in the internal carotid artery. Language testing was performed during the observation period of maximal amobarbital action as indicated by contralateral

brachial plegia. Patients were given the following tasks in the following order and up to four points were given, depending on the severity of the language disturbance: 0, no response; 1, meaningless utterance; 2, incorrect repetition or paraphasia; 3, self-correction; and 4, unimpaired.

The tasks were as follows:

1) Spontaneous counting. Patients were instructed to count, starting immediately before the amobarbital administration and continuously until the next task was given. If the patient could continue to count even after brachial plegia appeared, obvious speech arrest and no impairment indicate 0 and 4 points, respectively.
2) Letter reading. Patients were instructed to read aloud seven words consisting of three or four *Kana* letters. The maximum score was 28 points (seven items × four points).
3) Naming. Patients were asked to name aloud the five objects presented pictorially. The maximum score was 20 points (five items × four points).
4) Auditory comprehension. Patients were asked to carry out three simple tasks such as blinking eyes, opening the mouth, and raising the unparalyzed arm. The maximum score was 12 points (three items × four points).
5) Pointing objects. Patients were shown a picture with a set of four objects and were instructed to point to one chosen by the investigator (e.g., "Point to the cat."). The maximum score was 16 points (four items × four points).

Performance in Tasks 1 and 3 were considered to reflect the expressive language capabilities (maximum score, 24 points); performance in Tasks 2, 4, and 5 reflected receptive language functions (maximum score, 56 points).

RESULTS

Handedness and the Wada Test

Ninety-one patients (80 right-, eight left-, and three bilateral-handers) successfully underwent the Wada test. Language dominance was left, right, and bilateral hemispheres in 81, six, and four patients, respectively. The language dominance of the right-handed patients was left in 75 patients (93.8%), right in two patients (2.5%), and bilateral in three patients (including one patient with dissociated expression and receptive functions [3.8%]), respectively. For left-handed patients, four patients showed left and four showed right dominance. For both-handed patients, two showed left dominance and one bilateral (dissociated). These results were similar to those of previous reports on language dominance (3, 4).

For further analysis, we subdivided the subjects into groups with chronic epilepsy and with non-epilepsy. In the epilepsy group (n = 29), left, right, and bilateral dominance was 24 (82.8%), three (10.3%), and two (6.9%), respectively. In the non-epilepsy group (n = 62), left, right, and bilateral dominance was 57 (91.6%), four (6.4%), and one (1.6%), respectively.

fMRI with the Verb Generation Task

The verb generation task was designed to locate the expressive language area by fMRI. Among 117 patients who underwent the verb generation task, 100 patients (84.6%) completed the task and provided useful fMRI data. The results showed that the dominant hemisphere for the expressive language function was left, right, and bilateral in 90, eight, and two patients, respectively. In the epilepsy group (n = 34), left, right, and bilateral dominance was 29 (85.2%), three (8.8%), and two (8.5%), respectively. In the non-epilepsy group (n = 66), left, right, and bilateral dominance was 61 (92.4%), five (7.6%), and zero (0%), respectively. The activated regions on fMRI mainly involved the IFG and MFG, the lateral precG, AG, and the supplementary motor area (SMA) (*Figs. 1* and *2*).

In some patients, activations were observed in bilateral hemispheres. Except for two patients who showed bilateral dominance, the activations in the non-dominant hemisphere were restricted to MFG and precG and smaller in size, so the pixels did not reach a cluster significance (maximum values of Z-score, <2.2 or <10 pixels).

Compared with successful results of the Wada test, the successful rate of fMRI with the verb generation task was 90.1%. Seven patients with aphasia or dementia failed to complete the task. Three glioma patients with marked surrounding, four patients with brain ischemia and three patients with large arteriovenous malformations failed to exhibit significant activations in the frontal lobe (*Fig. 3*). These incomplete results are accounted for by the reported disadvantage of fMRI that data may be affected by the pathological changes of cerebral circulation (7, 10, 15).

fMRI with the A/C Categorization Task

The A/C categorization task was designed to locate the receptive language area by fMRI. Among 106 patients who performed the A/C categorization task, 71 (67.0%) completed the task and provided useful fMRI data. Compared with the verb generation task, the A/C categorization task more often activated wider areas in bilateral hemispheres (*Fig. 2*). Activations generally involved the bilateral frontal lobes, including the IFG, MFG, and precG, with laterality. The superior temporal regions, such as the STG and SmG, demonstrated activation spots in only 45% (n = 32) of the investigated patients, and the side predominance was not apparent in most cases. The fMRI data of the A/C categorization task were considered unsuitable to determine the receptive language areas and were not used for the final analyses.

Language MEG Profiles and Dipole Locations

The *Kana* reading task was designed to locate the receptive language area by MEG. The language MEG was performed in 117 patients, of whom 99 (85.4%) completed the task and provided useful data (*Figs. 1* and *2*). Results showed that the dominant hemisphere for the receptive language function was left, right, and bilateral in 85, 11, and three patients, respectively. In the epilepsy group (n = 31), left, right, and bilateral dominance was 26 (83.9%), three (9.7%), and two (6.5%), respectively. In the non-epilepsy group (n = 68), left, right, and bilateral dominance was 59 (86.8%), eight (11.8%), and one (1.5%), respectively.

Dipole clusters of late deflections localized mainly in the superior temporal region (STG, MTG, and SmG), and 60% of investigated patients also showed dipoles in the inferior tempo-

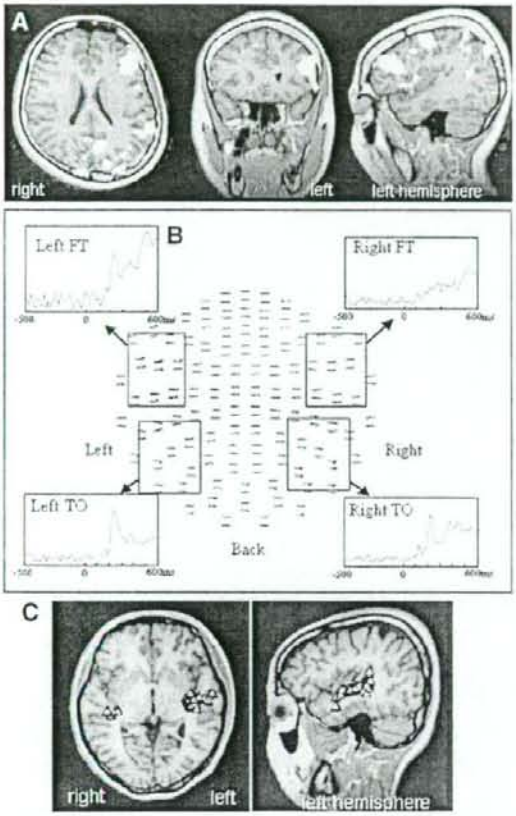

FIGURE 1. *A 24-year-old, right-handed man with epilepsy. A, fMRI with the verb generation task showing activations predominantly in the left IFG, MFG, PrecG, and parieto-occipital regions. B, square root mean field profiles of language MEG responses in the bilateral FT and TO regions. The left FT responses, peaking at 450 milliseconds, were markedly greater in amplitude than the right FT. C, source localization of the late deflections showing predominant dipole clusters (arrowheads) in the left superior temporal region. The left and right hemispheres contained 97 and 37 dipoles, respectively.*

ral region (FuG and inferior temporal gyrus). In 96 patients who showed unilateral language dominance, the total number of dipoles in the dominant versus non-dominant hemispheres was 124.1 ± 62.1 and 58 ± 30.9 (mean ± standard deviation), respectively. The ratio of the dipole number in the dominant hemisphere to the non-dominant hemisphere in each individual was 2.4 ± 1.7 (range, 1.43–14.4).

A typical result with all channels of MEG with the *Kana*-reading task is illustrated in *Figure 1*. Later deflections peaking at approximately 400 milliseconds were predominantly observed in the left FT. Bilateral TO regions demonstrated early deflections at approximately 200 milliseconds with short durations and little laterality. Estimated dipoles of the FT regions were densely accumulated in the left STG, MTG, and SmG (102 dipoles), whereas the right hemisphere showed fewer dipoles (54 dipoles) in the superior temporal region. This patient was thus determined to have receptive language dominance in the left temporal lobe.

The successful rate of language-MEG was 82.4%. Nine out of 39 epilepsy patients (23.1%) could not provide useful MEG data owing to artifacts from constant eye movements; the *Kana*-reading task was more difficult to complete than the verb generation task for patients with mental dysfunction. On the other hand, only one out of 18 AVM patients, owing to severe dyslexia, failed to provide useful MEG data, indicating that, in contrast to fMRI, MEG was not frequently affected by cerebral blood flow abnormalities (*Fig. 3*).

Combination of fMRI and MEG with Wada Test Verification

The verb generation task fMRI data depict expressive language areas well, but may be affected by cerebral blood flow abnormalities. The MEG results indicate receptive language areas well, but the task is rather complicated and may not be suited for patients with mental disorders. We sought to establish a non-invasive and reliable method to determine the laterality of language dominance by combining the advantages of these approaches. Furthermore, in terms of language functions, the results from fMRI and MEG can be integrated to locate expressive and receptive language areas and to provide reliable evidence whether or not there is dissociation. To verify the reliability of our method, 97 patients also underwent the Wada test.

Useful data from the method co-utilizing fMRI and MEG could be obtained from 87 out of 91 patients (95.6%). Remarkably, regarding language dominance, the results from the combination method matched the results of the Wada test in all 87 patients. Worth noting is that two patients (one with left temporal lobe epilepsy and the other with right insular astrocytoma) showed dissociated language areas using the combined method. The expressive language area was depicted in the left frontal lobe by fMRI, but the receptive language area was demonstrated in the right temporal lobe by MEG (*Fig. 4*). The Wada test results confirmed that both patients have language functions dissociated in the bilateral hemispheres. Among the 91 patients who underwent the Wada test, these were the only two patients in whom the Wada test detected dissociation of language functions.

In 12 epilepsy patients, the expressive and/or receptive language areas were electrophysiologically investigated via a subdural electrode implantation and the results were compared with those determined via the combined fMRI plus MEG method (*Fig. 5*). Out of eight patients who underwent cortical mapping for the expressive language area, all showed a speech arrest by electrical stimulation to the IFG and four to the MFG. All of the physiologically determined locations were confined within the areas depicted by the combined method. Out of six patients who received electrical stimuli to the temporal lobe,

four showed responses interpretable as impaired speech comprehension. In all such cases, the electrophysiologically determined location matched the area depicted by the combined method, although MEG-depicted receptive language areas covered relatively broad areas of the temporal lobe. The regions determined by the combined method were always broader, but had the border within the adjacent gyri of those determined by electrophysiological mapping.

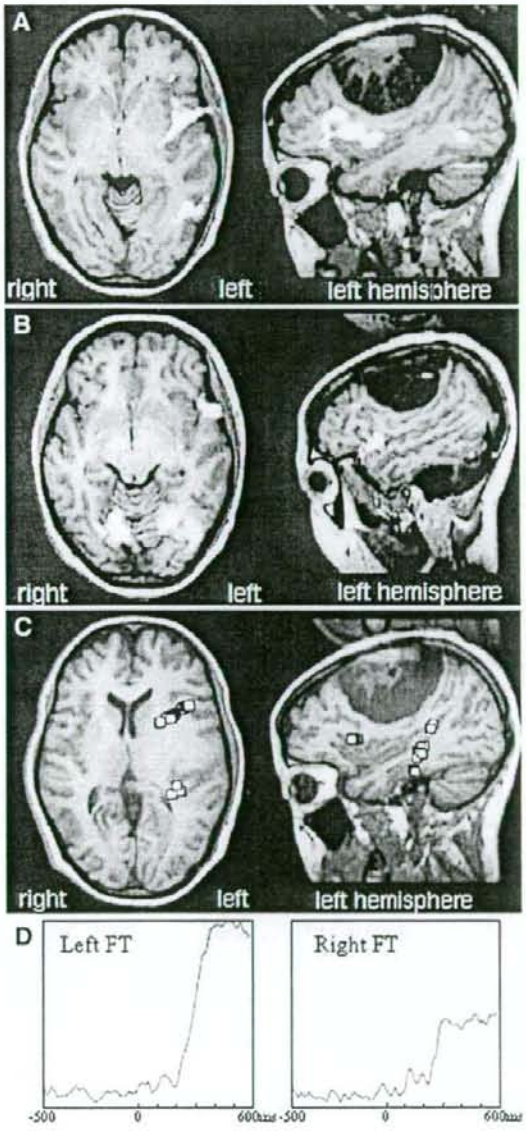

ILLUSTRATIVE CASES

Patient 1

A 16-year-old, right-handed female patient had experienced transient numbness in her left upper extremity with a 2-month history. T1-weighted MRI scans demonstrated an extra-axial cystic lesion in the left frontal region. Although the lesion markedly compressed the frontal lobe, she had no impairment of language and motor functions. fMRI with the verb generation task demonstrated obvious activation in the left IFG and MFG shifted inferiorly by the lesion (*Fig. 2A*). The A/C categorization task activated a small area of the left IFG, but mainly the bilateral occipital lobes. Concerning MEG with the *Kana* reading task, RMS of the left FT was much higher than that of the right, and numbers of semantic dipoles were 117 and 30 in left and right hemispheres, respectively. The main dipole clusters were located in the left IFG and STG. The tumor was totally removed and histopathological diagnosis was meningioma.

Patient 2

A 24-year-old, right-handed male patient had a large AVM in the left frontal lobe. fMRI detected little activation in the IFG or MFG, although a part of the left angular gyrus was activated by the verb generation task (*Fig. 3A*). MEG, however, disclosed numerous dipole accumulations in the left superior temporal region. In the MEG examination, the left and right hemispheres contained 130 and 45 dipoles, respectively, suggesting left language dominance (*Fig. 3B*). Auditory comprehension and letter-reading were suppressed by administration of amobarbital into the left carotid artery, although motor language function was preserved. These findings suggested that the steal effect caused by the AVM partly interfered with functional brain mapping of fMRI and the Wada test. In this case, MEG was helpful to decide language dominance (*Fig. 3*).

Patient 3

A 32-year-old, right-handed man experienced amnesia for several minutes. T1-weighted MRI scans and brain computed tomographic scans disclosed a hypointense and hypodense mass in the right insular cortex involving the surrounding white matter. Computed tomographic scans performed 6 years earlier, however, revealed no abnormality. These findings suggested that a low-grade astrocytoma might

FIGURE 2. *A 16-year-old, right-handed female patient with a large meningioma in the left frontal region. The patient had no impairment of language or motor functions.* A, *fMRI with the verb generation task showed activations mainly in the left IFG and MFG that shifted inferiorly by the tumor.* B, *fMRI with the abstract/concrete categorization task demonstrated activations in the bilateral occipital regions in addition to small active spots in the left IFG.* C, *square root mean field profiles of language-MEG responses demonstrated that the left FT responses, peaking at 400 milliseconds, were markedly larger in amplitude than the right FT.* D, *source localization of the late deflections showed predominant dipole clusters in the left posterior temporal region. The left and right hemispheres contained 117 and 30 dipoles, respectively. The combined fMRI plus MEG method indicated left language dominance, which was confirmed by Wada test.*

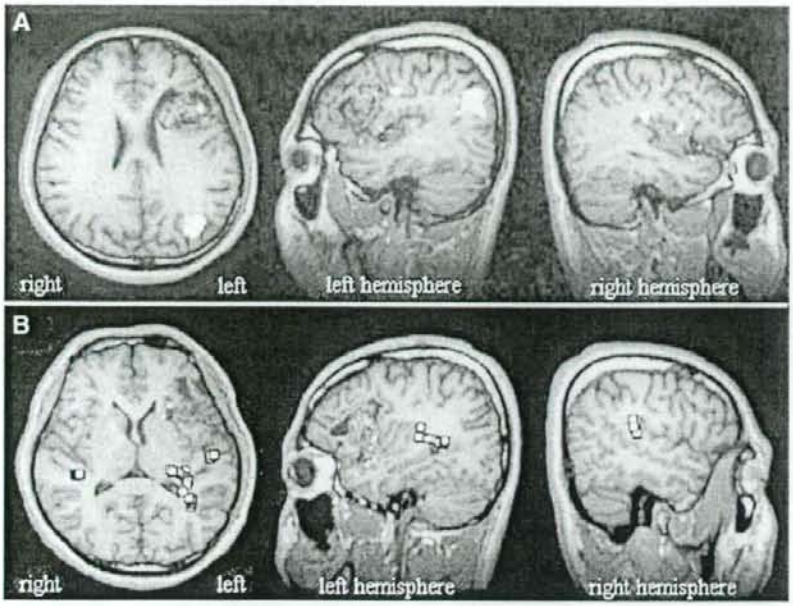

FIGURE 3. *A 24-year-old, right-handed man with a large AVM in the left frontal lobe.* A, *fMRI with the verb generation task showed little activation in the left frontal lobe where the AVM was located.* B, *source localization of the late FT and TO deflections on MEG showed predominant dipole clusters in the left posterior STG. The left and right hemispheres contained 123 and 51 dipoles, respectively.*

have slowly developed during the past 6 years. In the results of the verb generation task, the left hemisphere had obvious activations in the IFG, MFG, precG, and the angular gyrus, indicating that this patient had left dominance of motor-language functions (*Fig. 4A*). In contrast, estimated dipoles of the FT responses were concentrated in the posterior part of the right STG and MTG (138 dipoles) and another dipole cluster (64 dipoles) of the TO region was localized in the right FuG. The total dipole number of the left hemisphere (48 dipoles) did not reach even a quarter of that of the right hemisphere, suggesting right-sided dominance of temporal language functions (*Fig. 4*).

During the Wada test, he stopped counting (0 out of 4 points; 0%) and failed to name objects (6 out of 20 points; 30%) after left intracarotid injection, whereas letter-reading (21 out of 28 points; 75%), auditory comprehension (12 out of 12 points, 100%), and pointing objects tasks (16 out of 16 points; 100%) were well preserved. In contrast, after right intracarotid injection, letter reading (13 out of 28 points; 45%), auditory comprehension (3 out of 12 point; 25%), and pointing objects (4 out of 16 points; 25%) tasks were markedly suppressed, although he continued to count correctly without speech blockade (4 out of 4 points; 100%) and could perform naming (17 out of 20 points; 85%). These findings suggested that language functions were distributed separately over the bilateral hemispheres, and the expressive and receptive language functions were dissociated in the left frontal and right temporal lobes, respectively. A striking fact was that the combination of fMRI and MEG predicted the special profiles of language functions noninvasively.

DISCUSSION

We demonstrated that our method using both fMRI with the verb generation task and MEG with the *Kana* reading task is highly reliable in determining the language dominance in patients with brain lesions. The accuracy of the dominance laterality was confirmed by a 100% match with the results from the Wada test. fMRI and MEG compensated each other's disadvantages. The tasks of fMRI were rather simple and could be accomplished even by patients with mental dysfunctions, whereas MEG results were seldom affected by cerebral blood flow abnormalities. Reliable data on language functions were also obtained by combining the advantageous features of fMRI and MEG. fMRI with the verb generation task well depicted the expressive language area as activations in the frontal lobe, most commonly in the IFG. MEG, on the other hand, showed dipole clusters predominantly in the superior temporal regions representing the receptive language area. In the epilepsy group, left and bilateral dominance were approximately 85% and more than 6%, respectively, whereas, in the non-epilepsy group, left and bilateral dominance were more than 90% and less than 2%, respectively. The combined method, including the Wada test, fMRI, and MEG, clearly demonstrated bilateral dominance is more often observed in the epilepsy group than in the non-epilepsy group.

In our study, two out of 87 patients analyzed (2.3%) were found to have dissociation of the expressive and receptive language functions by co-utilization of fMRI and MEG, verified by the Wada test, which best described the usefulness of our method in identifying the areas of the two language functions separately. In both cases, neither modality alone demonstrated the dissociation. Although several cases have been reported that dissociated language functions were found by fMRI, none of those was proven by the Wada test (2, 8, 21, 23). Our results show that neither fMRI nor MEG alone is sufficient to accurately locate the expressive and receptive language areas, and the combined use is the key to obtaining high reliability.

The results from electrophysiological investigation via a subdural electrode implantation in 12 patients further confirmed the accuracy of the present method. Pouratian et al. (22) reported that the sensitivity and specificity of language-fMRI

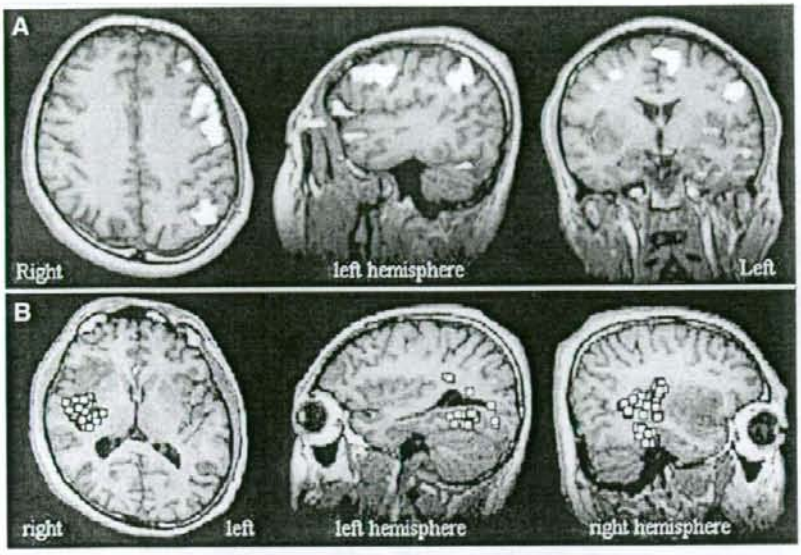

FIGURE 4. *A 32-year-old, right-handed man with astrocytoma in the right insular cortex and the surrounding white matter. A, fMRI with the verb generation task showed main activations in the IFG, MFG, precG, and AG, indicating left dominance of the expressive language function. B, in contrast to the fMRI results, source localization of the late FT deflections on MEG showed predominant dipole clusters in the right temporal lobe. The left and right hemispheres contained 48 and 202 dipoles, respectively. The combined fMRI plus MEG method thus indicated dissociated frontal motor and temporal receptive language functions. This result was confirmed by the Wada test. The patient showed impaired counting and object naming after amobarbitol injection into the left carotid artery. In contrast, letter reading, auditory comprehension and object pointing tasks were markedly suppressed, without counting impairment and speech blockade, after amobarbitol injection into the right carotid artery.*

were dependent on the task, lobe, and matching criterion. The sensitivity and specificity of fMRI activations during expressive linguistic tasks in the frontal lobe were found to be up to 100 and 66.7%, respectively, in the frontal lobe. FitzGerald et al. (6) reported that sensitivity and specificity for all multiple language tasks ranged from 81 to 53% (6). On the other hand, several groups have reported that the language map obtained from fMRI poorly matched the intraoperative electrical stimulation mapping (6, 25). In our study of language-fMRI, every electrical stimuli to the IFG, where the fMRI-activation was observed, caused speech arrest. However, the stimulation to MFG caused language-related symptoms in only half of patients. Although the sensitivity of fMRI might be high, there are still several issues of individual variability of fMRI activation and semantic tasks. The discrepancy can be partly accounted for by the fundamental differences in methodology such that the electrical stimulation directly blocks the specific language functions, whereas fMRI picks up all activated areas involved in the language tasks. Therefore, fMRI-based mapping largely depends on the design of the performing task. We tested two different tasks for fMRI and found the verb generation task better suited for language mapping than the A/C categorization task. The significance of activations depicted on fMRI is still under debate. Language-fMRI activations may be related to various semantic components of the task, including the will to retrieve verbal materials and the memory related to articulations. Despite that the A/C categorization task was designed to detect the receptive language area, activations in the temporoparietal region was less frequently observed than in the frontal region. Neural activities in the temporoparietal area are considered relatively scarce (25), and the discrepant activities of the frontal and temporoparietal regions may be owing to physiological variations of brain regions. Alternatively, the frontal and temporal lobes may have different oscillations (brain rhythms) of brain activity in response to verbal tasks, which are reflected in changes in neuronal currents and cerebral blood flow.

Our study demonstrated that dominance of the receptive language function could be accurately determined by MEG. For that purpose, we originally designed the task of three-letter word reading and silent categorization and used the dipoles calculated from late deflections to process the MEG results. It has been reported that cortical evoked potentials recorded by subdural electrodes showed responses at approximately 200 (early) and 400 (late) milliseconds in the left temporal lobe cortex after letter presentation (1, 17). The late potentials have been noted especially in tasks involving decisions based on visually presented words (13, 14). In this study, the sources of late responses (250–600 ms) were located mostly in the posterior temporal region, and the laterality of dipole clusters accurately reflected the receptive language dominance. It has been reported that dipoles in the superior temporal region showed an excellent agreement with an intraoperative electrical mapping (27). We also included dipoles in the FuG for language dominance determination based on our experience with a case in which an injury of FuG resulted in pure dyslexia (12). These contrivances in our method may have led to improvement in accuracy on language dominance determination over previous reports (20). Basic technical issues of the MEG investigation still remain. Eye movement artifacts were strong enough to distort the baseline of the MEG data. In our study,

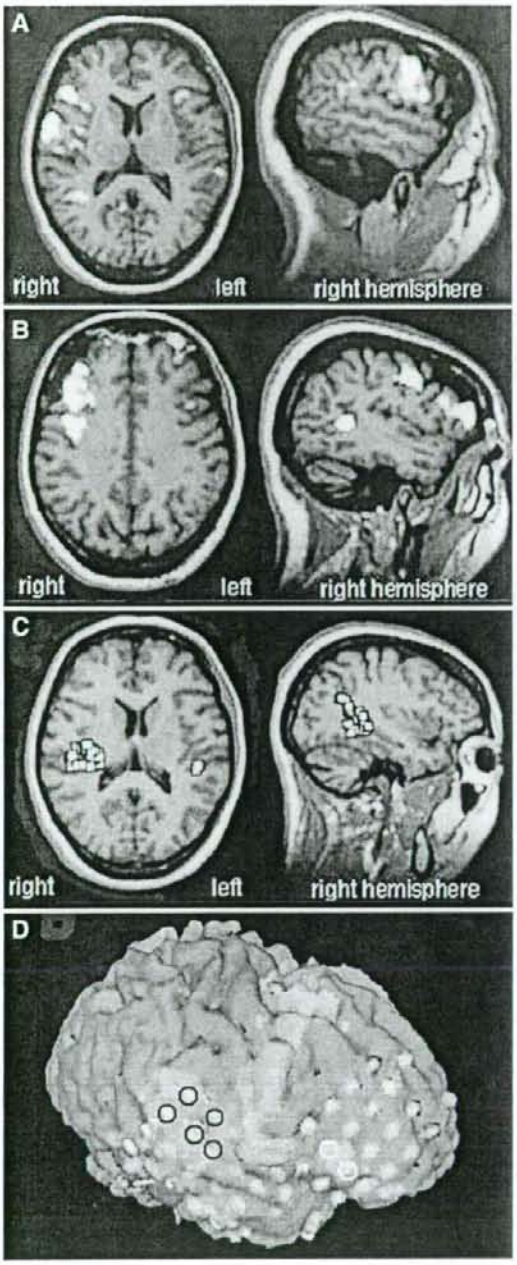

we asked patients to keep gazing at the center of the screen during the semantic decision without blinking. As a result, artifacts were observed at later than 600 milliseconds after letter presentation and usually did not affect the early and late semantic responses. It is, however, important to prevent artifacts by monitoring eye movements and using rejection thresholds.

In conclusion, by co-utilizing fMRI and MEG, we established a method to determine language dominance with a high reliability. The fMRI activations with the verb generation task identified the expressive language area, whereas the language MEG dipoles located the receptive language areas. Our institution is now routinely using the combined technique to identify the language dominance. If it does not produce data on cerebral dominance, we additionally perform the Wada test before surgery. This non-invasive and repeatable method may be an effective alternative to the Wada test and may be useful in the management of patients with brain lesions.

Disclosure

This work was supported in part by the Japan Epilepsy Research Foundation, Takeda Promotion of Science Foundation, a grant-in-aid No.17591502 for scientific research from MEXT, a Research Grant of the Princess Takamatsu Cancer Research Fund, Terumo Promotion of Science Foundation, Brain Science foundation, and Grant-in-Aid No. 18020010 for Scientific Research on Priority Areas Integrative Brain Research from MEXT.

REFERENCES

1. Allison T, McCarthy G, Nobre A, Puce A, Belger A: Human extrastriate visual cortex and the perception of faces, words, numbers, and colors. **Cereb Cortex** 4:544–554, 1994.
2. Baciu MV, Watson JM, McDermott KB, Wetzel RD, Attarian H, Moran CJ, Ojemann JG: Functional MRI reveals an interhemispheric dissociation of frontal and temporal language regions in a patient with focal epilepsy. **Epilepsy Behav** 4:776–780, 2003.
3. Branch C, Milner B, Rasmussen T: Intracarotid sodium amytal for the lateralization of cerebral speech dominance: Observations in 123 patients. J **Neurosurg** 21:399–405, 1964.
4. Brazdil M, Zakopcan J, Kuba R, Fanfrdlova Z, Rektor I: Atypical hemispheric language dominance in left temporal lobe epilepsy as a result of the reorganization of language functions. **Epilepsy Behav** 4:414–419, 2003.
5. Chen HM, Varshney PK: Mutual information-based CT-MR brain image registration using generalized partial volume joint histogram estimation. **IEEE Trans Med Imaging** 22:1111–1119, 2003.

FIGURE 5. *A 40-year-old, left-handed woman with epilepsy. A, fMRI with the verb generation task showed activations predominantly in the right IFG and MFG. B, fMRI with the A/C categorization task demonstrated activations in the right MFG and the posterior STG. C, source localization of the late deflections on MEG showed predominant dipole clusters (white squares) in the right posterior temporal region. The left and right hemispheres showed 44 and 144 dipoles, respectively. D, three-dimensionally reconstructed MRI scans fused with activation of the verb generation-fMRI (orange) and dipoles of language-MEG (blue). After implantation of subdural electrodes (gold), cortical mapping was performed with 50Hz bipolar electrical stimulation. Stimulation with intensity of 7mA to the right IFG caused speech arrest (white circles), whereas stimulation to the posterior STG caused impairment of auditory comprehension and reading capability (black circles).*

6. FitzGerald DB, Cosgrove GR, Ronner S, Jiang H, Buchbinder BR, Belliveau JW, Rosen BR, Benson RR: Location of language in the cortex: A comparison between functional MR imaging and electrocortical stimulation. **AJNR Am J Neuroradiol** 18:1529–1539, 1997.
7. Holodny AI, Schulder M, Liu WC, Maldjian JA, Kalnin AI: Decreased BOLD functional MR activation of the motor and sensory cortices adjacent to a glioblastoma multiforme: Implications for image-guided neurosurgery. **AJNR Am J Neuroradiol** 20:609–612, 1999.
8. Holodny AI, Schulder M, Ybasco A, Liu WC: Translocation of Broca's area to the contralateral hemisphere as the result of the growth of a left inferior frontal glioma. **J Comput Assist Tomogr** 26:941–943, 2002.
9. Janszky J, Ollech I, Jokeit H, Kontopoulou K, Mertens M, Pohlmann-Eden B, Ebner A, Woermann FG: Epileptic activity influences the lateralization of mesiotemporal fMRI activity. **Neurology** 63:1813–1817, 2004.
10. Kamada K, Houkin K, Iwasaki Y, Takeuchi F, Kuriki S, Mitsumori K, Sawamura Y: Rapid identification of the primary motor area by using magnetic resonance axonography. **J Neurosurg** 97:558–567, 2002.
11. Kamada K, Kober H, Saguer M, Moller M, Kaltenhauser M, Vieth J: Responses to silent Kanji reading of the native Japanese and German in task subtraction magnetoencephalography. **Brain Res Cogn Brain Res** 7:89–98, 1998.
12. Kamada K, Sawamura Y, Takeuchi F, Houkin K, Kawaguchi H, Iwasaki Y, Kuriki S: Gradual recovery from dyslexia and related serial magnetoencephalographic changes in the lexicosemantic centers after resection of a mesial temporal astrocytoma. Case report. **J Neurosurg** 100:1101–1106, 2004.
13. Kutas M, Hillyard SA: Reading senseless sentences: Brain potentials reflect semantic incongruity. **Science** 207:203–205, 1980.
14. Kutas M, Hillyard SA: Brain potentials during reading reflect word expectancy and semantic association. **Nature** 307:161–163, 1984.
15. Lehericy S, Biondi A, Sourour N, Vlaicu M, du Montcel ST, Cohen L, Vivas E, Capelle L, Faillot T, Casasco A, Le Bihan D, Marsault C: Arteriovenous brain malformations: Is functional MR imaging reliable for studying language reorganization in patients? Initial observations. **Radiology** 223:672–682, 2002.
16. Lehericy S, Cohen L, Bazin B, Samson S, Giacomini E, Rougetet R, Hertz-Pannier L, Le Bihan D, Marsault C, Baulac M: Functional MR evaluation of temporal and frontal language dominance compared with the Wada test. **Neurology** 54:1625–1633, 2000.
17. Nobre AC, Allison T, McCarthy G: Word recognition in the human inferior temporal lobe. **Nature** 372:260–263, 1994.
18. Oldfield RC: The assessment and analysis of handedness: The Edinburgh inventory. **Neuropsychologia** 9:97–113, 1971.
19. Papanicolaou AC, Simos PG, Breier JI, Zouridakis G, Willmore LJ, Wheless JW, Constantinou JE, Maggio WW, Gormley WB: Magnetoencephalographic mapping of the language-specific cortex. **J Neurosurg** 90:85–93, 1999.
20. Papanicolaou AC, Simos PG, Castillo EM, Breier JI, Sarkari S, Pataraia E, Billingsley RL, Buchanan S, Wheless J, Maggio V, Maggio WW: Magnetocephalography: A noninvasive alternative to the Wada procedure. **J Neurosurg** 100:867–876, 2004.
21. Petrovich NM, Holodny AI, Brennan CW, Gutin PH: Isolated translocation of Wernicke's area to the right hemisphere in a 62-year-man with a temporoparietal glioma. **AJNR Am J Neuroradiol** 25:130–133, 2004.
22. Pouratian N, Bookheimer SY, Rex DE, Martin NA, Toga AW: Utility of preoperative functional magnetic resonance imaging for identifying language cortices in patients with vascular malformations. **Neurosurg Focus** 13:E4, 2002.
23. Ries ML, Boop FA, Griebel ML, Zou P, Phillips NS, Johnson SC, Williams JP, Helton KJ, Ogg RJ: Functional MRI and Wada determination of language lateralization: A case of crossed dominance. **Epilepsia** 45:85–89, 2004.
24. Roux FE, Boulanouar K, Lotterie JA, Mejdoubi M, LeSage JP, Berry I: Language functional magnetic resonance imaging in preoperative assessment of language areas: Correlation with direct cortical stimulation. **Neurosurgery** 52:1335-1345, 2003.
25. Rutten GJ, Ramsey NF, van Rijen PC, Noordmans HJ, van Veelen CW: Development of a functional magnetic resonance imaging protocol for intraoperative localization of critical temporoparietal language areas. **Ann Neurol** 51:350–360, 2002.
26. Rutten GJ, Ramsey NF, van Rijen PC, van Veelen CW: Reproducibility of fMRI-determined language lateralization in individual subjects. **Brain Lang** 80:421–437, 2002.
27. Simos PG, Papanicolaou AC, Breier JI, Wheless JW, Constantinou JE, Gormley WB, Maggio WW: Localization of language-specific cortex by using magnetic source imaging and electrical stimulation mapping. **J Neurosurg** 91:787–796, 1999.
28. Woermann FG, Jokeit H, Luerding R, Freitag H, Schulz R, Guertler S, Okujava M, Wolf P, Tuxhorn I, Ebner A: Language lateralization by Wada test and fMRI in 100 patients with epilepsy. **Neurology** 61:699–701, 2003.
29. Yetkin FZ, Mueller WM, Morris GL, McAuliffe TL, Ulmer JL, Cox RW, Daniels DL, Haughton VM: Functional MR activation correlated with intraoperative cortical mapping. **AJNR Am J Neuroradiol** 18:1311–1315, 1997.

COMMENTS

This is an interesting article evaluating the complementary features of functional magnetic resonance imaging (fMRI) and magnetoencephalography (MEG) to assess language lateralization in 87 patients. Whereas any test of language lateralization is suspect if 100% correlation is found, the authors have carefully described their techniques and the analysis of results. It is quite apparent that fMRI with verb generation tasks is best at activating anterior language areas, whereas abstract versus concrete naming tasks can be less robust. This is a good article and a large experience worthy of publication.

G. Rees Cosgrove
Burlington, Massachusetts

The authors have applied fMRI and MEG techniques to localize speech function in a large number of patients with different brain lesions. They were able to supplement the two noninvasive tests with the Wada test in 80% of the patients. They were able to obtain useful data with the co-utilization of fMRI and MEG in 95.6% of the patients and found a somewhat surprisingly good match with the results of the Wada test in 100% of those. In the results section, the authors discuss a few differences to the localization of language areas by electrophysiological means. They point out the fact that atypical language dominance or bilateral language representation is more frequent in patients with chronic epilepsy than in those without epilepsy. This is an important fact not known to many neurosurgeons who are not ordinarily involved with epilepsy cases. The results of this study make it more likely that, in the future, the invasive Wada test procedure might be abolished in those institutions at which MEG is available. This constitutes a notable limitation of this noninvasive technique. If fMRI is used alone, the success rate for obtaining useful data is 84.6% for word generation tasks and only 67% for the abstract/concrete categorization task. This is quite an interesting study and the results are very promising; however, the limitations are not economical. A number of patients cannot complete all the tasks necessary for fMRI study, and MEG studies can be disturbed by eye movement artifacts. We look forward to other reports confirming these promising results.

Johannes Schramm
Bonn, Germany

The authors present some very interesting data in the realm of functional imaging to determine cerebral dominance for language. Currently, the standard modality for determining cerebral dominance is the venerable Wada test. In this study, the authors use both MEG and fMRI to determine language dominance based on activation in the inferior frontal gyrus and middle frontal gyrus using fMRI and dipole moments reflecting or indicating receptive language fields in the temporal lobe. As expected, they had some difficulty with the fMRI data owing to the underlying deficit in the patient, which suggests that fMRI is not always as good as one might expect in terms of determin-

ing cerebral dominance using a verb generation silent language task. We know that fMRI is not a good choice for defining receptive language fields that correspond to intraoperative stimulation mapping. However, when fMRI was used together with MEG, the authors were able to demonstrate 100% concordance with data from the Wada test. Thus, this is a very important study indicating that, in the near future, it may be possible to bypass the Wada test with these two powerful functional imaging modalities. That being said, not every institution is going to be able to obtain both of these functional tests. Therefore, it is unlikely that this strategy is going to replace Wada tests completely. Yet, this is a very important line of investigation and a novel observation that points out the frailties of functional imaging for cerebral dominance localization and the potential power when the different functional tests are combined.

Mitchel S. Berger
San Francisco, California

Portrait of James Figg (1695–1734), by William Hogarth. (1697–1764). Acknowledged in Britain as the "Father of Boxing," Figg popularized the sport with teaching and exhibitions and, following victories over all the other British contenders, declared himself "heavyweight champion of England" in 1719.

FAMILIAL OCCURRENCE OF DYSEMBRYOPLASTIC NEUROEPITHELIAL TUMOR-LIKE NEOPLASM OF THE SEPTUM PELLUCIDUM: CASE REPORT

Taiichi Saito, M.D., Ph.D.

Department of Neurosurgery,
Graduate School of Biomedical Sciences,
Hiroshima University,
Hiroshima, Japan

Kazuhiko Sugiyama, M.D., Ph.D.

Department of Neurosurgery,
Graduate School of Biomedical Sciences,
Hiroshima University,
Hiroshima, Japan

Fumiyuki Yamasaki, M.D., Ph.D.

Department of Neurosurgery,
Graduate School of Biomedical Sciences,
Hiroshima University,
Hiroshima, Japan

Atsushi Tominaga, M.D., Ph.D.

Department of Neurosurgery,
Graduate School of Biomedical Sciences,
Hiroshima University,
Hiroshima, Japan

Kaoru Kurisu, M.D., Ph.D.

Department of Neurosurgery,
Graduate School of Biomedical Sciences,
Hiroshima University,
Hiroshima, Japan

Yukio Takeshima, M.D., Ph.D.

Department of Pathology,
Graduate School of Biomedical Sciences,
Hiroshima University,
Hiroshima, Japan

Takanori Hirose, M.D., Ph.D.

Department of Pathology,
Saitama Medical University School
of Medicine,
Moroyama, Japan

Reprint requests:
Taiichi Saito, M.D., Ph.D.,
Department of Neurosurgery,
Graduate School of Biomedical Sciences,
Hiroshima University,
1-2-3 Kasumi, Minami-ku,
Hiroshima 734-8551, Japan.
Email: taiichi@hiroshima-u.ac.jp

Received, July 2, 2007.
Accepted, April 21, 2008.

OBJECTIVE: Dysembryoplastic neuroepithelial tumor (DNT)-like neoplasms of the septum pellucidum are extremely rare. In this article, we report the familial occurrence of these neoplasms.

CLINICAL PRESENTATION: We report two cases of such neoplasms: Patient 1, a 42-year-old woman, and Patient 2, the 20-year-old nephew of Patient 1. Patient 1 experienced headache and worsening dizziness; Patient 2 experienced headache and worsening dizziness and also had partial seizures. In both cases, magnetic resonance imaging (MRI) revealed an intraventricular tumor adjacent to the septum pellucidum. Both tumors appeared as a hypointense region on T1-weighted MRI, and both appeared as a hyperintense region on T2-weighted MRI without gadolinium enhancement. Interestingly, both tumors had a high apparent diffusion coefficient.

INTERVENTION: Both tumors were subtotally removed and had common histological findings, such as alveolar structures with oligodendroglia-like cells and "specific glioneuronal element." These findings are consistent with a dysembryoplastic neuroepithelial tumor-like neoplasm. After tumor removal, the symptoms disappeared. The postoperative course was uneventful, and the patients did not require adjuvant therapy. MRI showed no regrowth of residual tumors at 4 years (Patient 1) and 2 years (Patient 2) postoperatively.

CONCLUSION: The familial occurrence of this rare tumor suggests that both of these cases arose from a common germline mutation. Identification of this rare tumor in this rare location is important to avoid unnecessary adjuvant therapy. A markedly high apparent diffusion coefficient and histological findings of specific glioneuronal element can facilitate the differential diagnosis of dysembryoplastic neuroepithelial tumor-like neoplasms. Genetic study of affected patients in this family may provide clues to its molecular pathogenesis.

KEY WORDS: Dysembryoplastic neuroepithelial tumor, Familial occurrence, Intraventricular neoplasms, Neuroendoscopy, Septum pellucidum

Neurosurgery 63:E370-E372, 2008 DOI: 10.1227/01.NEU.0000330421.62353.63 www.neurosurgery-online.com

Dysembryoplastic neuroepithelial tumor (DNT) is a clinicopathologically unique tumor, located mostly in the cerebral cortex and associated with a long-standing history of seizure in younger patients. DNT is characterized by its intracortical location and multinodularity. The typical histological features are heterogeneous cellular composition including oligodendroglia-like cells (OLC) and, to a lesser extent, astrocytes and neurons, specific glioneuronal elements composed of OLCs and floating neurons in mucoid stroma (3, 4). However, there have been reported cases of DNTs in uncommon locations (2, 6, 8, 12, 13, 18).

Abbreviations: ADC, apparent diffusion coefficient; CGH, comparative genomic hybridization; CT, computed tomography; DNT, dysembryoplastic neuroepithelial tumor; MRI, magnetic resonance imaging; OLC, oligodendroglia-like cell

DNT-like neoplasms of the septum pellucidum are extremely rare and were first reported by Baisden et al. (1) in 2001. These tumors originate from the septum pellucidum

around the foramen of Monro, extend into the lateral or third ventricles, and have many of the histopathological features of DNT. The rarity of these tumors can lead to a misdiagnosis of other intraventricular tumors. In this article, we report two cases (a 42-year-old woman and her 20-year-old nephew) of tumors that were histologically confirmed to be DNT-like neoplasms of the septum pellucidum. This appears to be the first known familial occurrence of this type of tumor.

CASE REPORTS

Patient 1

A 42-year-old woman had been experiencing headache and worsening dizziness for 10 years. Magnetic resonance imaging (MRI) revealed an intraventricular non-contrast-enhancing mass. The patient was referred to our department in June 2002. General and neurological examination findings were normal. Computed tomography (CT) revealed an intraventricular low-density mass, with mild enlargement of the left lateral ventricle (*Fig. 1A*). The mass was hypointense on T1-weighted MRI (*Fig. 1B*) and markedly hyperintense on T2-weighted MRI (*Fig. 1C*). Gadolinium injection did not result in enhancement (*Fig. 1, D* and *E*). Coronal images showed that the tumor was attached to the anteroinferior part of the septum pellucidum, extending into the lateral ventricle and the third ventricle through the left foramen of Monro (*Fig. 1E*). The lesion was hypointense on diffusion-weighted imaging and had a high apparent diffusion coefficient (ADC) (2.534×10^{-3} mm^2/s) (*Fig. 1F*). In July 2002, the patient underwent left frontal craniotomy for removal of the tumor, using the transcortical transventricular approach. We first examined the tumor using a neuroendoscope. The tumor was pinkish-white and had a smooth surface. It was attached to the anteroinferior part of the septum pellucidum and occupied the foramen of Monro (*Fig. 2A*). After neuroendoscopic observation, we removed the tumor subtotally because of the adhesion of the tumor to the anterior septal vein. The tumor was soft and hypovascular and was easily aspirated. Histological examination revealed an alveolar structure with OLCs, a fibrillary matrix (*Fig. 2B*), and several occurrences of a rosette-like pattern. No perivascular pseudorosettes were seen. Furthermore, some of the alveolar structures had specific glioneuronal elements with OLCs, floating neurons, and mucoid stroma (*Fig. 2C*). No typical multiple discrete microscopic nodules were observed. Immunohistochemical staining revealed that OLCs were positive for S-100 protein but negative for glial fibrillary acidic protein and synaptophysin. Some of the matrix and floating neurons were positive for neurofilament, but the OLCs were negative (*Fig. 2D*). Rosette-like formations were negative for epithelial membrane antigen. The MIB-1 (Ki-67) index was 0.3%. Electron microscopic analysis revealed that the tumor cell did not have cilia and microvilli at the lateral surface (*Fig. 2E*). Although internal nodular architecture was not present, these findings suggested that this tumor was composed of DNT-like tissues. The patient did not undergo any adjuvant therapy. Her headache and dizziness disappeared after the surgery, and she had an uneventful postoperative course. Four years postoperatively, MRI showed no further growth of the residual tumor (*Fig. 2F*).

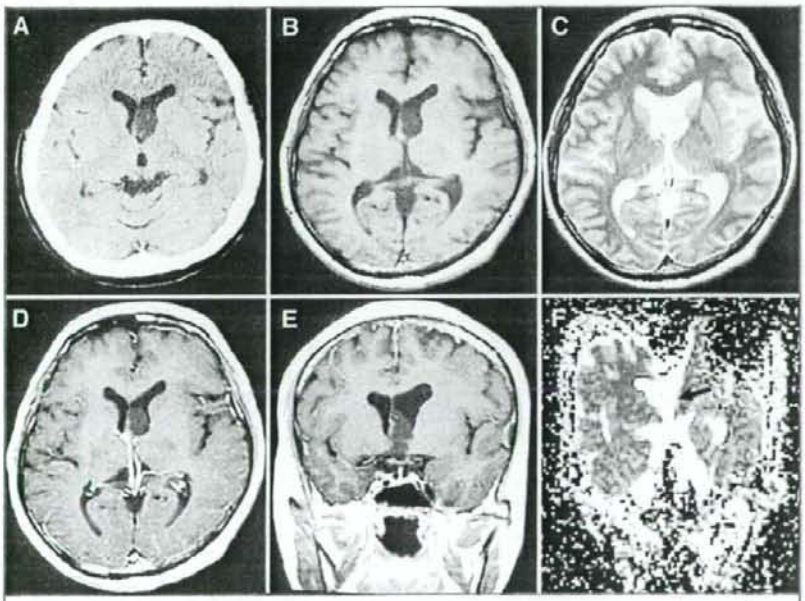

FIGURE 1. A, *plain computed tomography (CT) revealing an intraventricular low-density mass adjacent to the septum pellucidum.* B–F, *magnetic resonance imaging (MRI) scans before surgery. The intraventricular mass is hypointense on T1-weighted (B) and hyperintense on T2-weighted (C) MRI scans. Axial (D) and coronal (E) T1-weighted MRI scans with gadolinium showing no enhancement of the mass in the left lateral and third ventricle. F, the mass is hyperintense on coronal section of apparent diffusion coefficient map image.*

Patient 2

A 20-year-old man, a nephew of Patient 1 (*Fig. 3*), had been experiencing headache and dizziness for 3 years, and had been experiencing focal seizures for 1 year. He was referred to our department in May 2004, after MRI revealed a non-contrast-enhancing mass in the third ventricle. General and neurological examination findings were normal. However, on electroencephalography, sporadic spikes and waves were observed, with a focus on the right frontal lobe. CT revealed mild enlargement of the right lateral ventricle with an intraventricular low-density mass (*Fig. 4A*). The lesion was hypointense on T1-weighted MRI (*Fig. 4B*) and hyperintense on T2-weighted MRI (*Fig. 4C*). Gadolinium injection did not result in enhancement (*Fig. 4D*). In coronal images, the tumor was attached to the anteroinferior part of the septum pellucidum and occupied the anterior part of the third ventricle (*Fig. 4E*). The lesion was hypointense on diffusion-

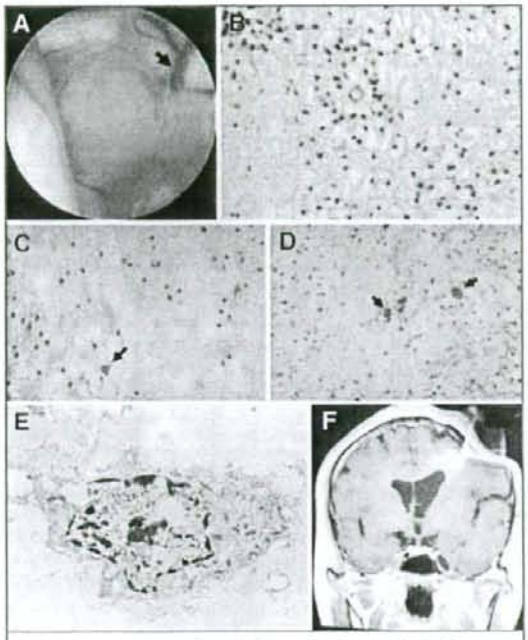

FIGURE 2. A, *neuroendoscopic image showing a pinkish-white mass with a smooth surface in the left anterior horn. The mass is attached to the septum pellucidum and involves the left anterior septal vein (arrow).* B–D, *hematoxylin and eosin staining showing an alveolar architecture with oligodendroglia-like cells (OLC) (original magnification, ×400) and (C and D) specific glioneuronal elements with floating neurons (arrows).* D, *floating neurons (arrows) are positive for neurofilament, but OLCs are negative.* E, *electron microscopy showing that the tumor cell does not have cilia and microvilli at the lateral surface.* F, *postoperative T1-weighted MRI showing no regrowth of residual tumor.*

weighted imaging and had a high ADC (2.821×10^{-3} mm^2/s) (*Fig. 4F*). In June 2004, the patient underwent right frontal craniotomy, and the tumor was removed using a transcortical transventricular approach. Neuroendoscopic examination showed that the tumor was pinkish-white and occupied the right foramen of Monro (*Fig. 5A*). We removed the tumor subtotally. The tumor was grossly similar to that of Patient 1 and was easily aspirated. Histological examination showed an alveolar structure like that of the tumor in Patient 1, with several occurrences of a rosette-like pattern (*Fig. 5B*). No perivascular pseudorosettes were seen. Some of the alveolar structures had specific glioneuronal elements with floating neurons (*Fig. 5B*). No typical multiple, discrete microscopic nodules were observed. Immunohistochemical staining revealed that OLCs were positive for S-100 protein but negative for glial fibrillary acidic protein (*Fig. 5C*) and synaptophysin. Some of the matrix was positive for glial fibrillary acidic protein, suggesting the presence of reactive astrocytes (*Fig. 5C*). Other parts of the matrix and some of the floating neurons were positive for neurofilament, but the OLCs were negative (*Fig. 5D*). Rosette-like formations were negative for epithelial membrane antigen. The MIB-1 (Ki-67) index was 0.2%. These histological findings were similar to those of the tumor in Patient 1. The patient did not undergo any adjuvant therapy. His headache and seizures disappeared after surgery, and he had an uneventful postoperative course. The sporadic spikes and waves on electroencephalography also disappeared, although the mechanism for this result is unknown. Two years postoperatively, MRI showed no regrowth of the residual tumor (*Fig. 5E*).

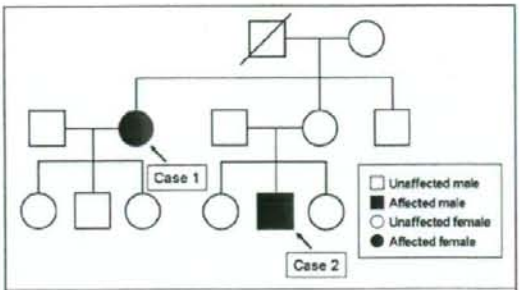

FIGURE 3. *Simplified pedigree of the family with two patients affected by dysembryoplastic neuroepithelial tumor-like neoplasms of the septum pellucidum. Patient 2 is a maternal nephew of Patient 1.*

DISCUSSION

Although most DNTs occur in the supratentorial cerebral cortex (3, 4), there have been reported cases of DNTs in uncommon locations such as the pons (14), midbrain (13), thalamus (16), and cerebellum (6, 12, 14, 18). Daumas-Duport et al. (4) suggested that DNTs in these location are related to the secondary germinal layers, in accordance with their hypothesis of histogenesis of DNT. Furthermore, Baisden et al. (1) and Cervera-Pierot et al. (2) demonstrated that DNTs or DNT-like neoplasms can arise within the septum pellucidum. Recently, Harter et al. (8) also reported a DNT located in the septum pellucidum. In the present report, we describe the first known familial occurrence of DNT-like neoplasm of the septum pellucidum. Given the low incidence of these tumors, this familial occurrence is of great interest. We assume that these previously reported tumors and the present tumors belong to the same category and have similar biological behavior. These tumors occurred in relatively young patients (mean age, 22.7 yr; range, 6–42 yr), and most of them were attached to the anteroinferior septum pellucidum, around the foramen of Monro. Consequently, some of them presented with obstructive hydrocephalus. Although neither the present tumors nor the previously reported tumors exhibited internal nodular structure, they had other features of DNT, including "specific glioneuronal elements" with OLCs, "floating neurons," and mucoid stroma (11). Although the present patients and all but one of the previously reported patients with this tumor did not undergo any postoperative adjuvant therapy, they did not show signs of recurrence or regrowth of residual tumors. These observations suggest that these tumors can be

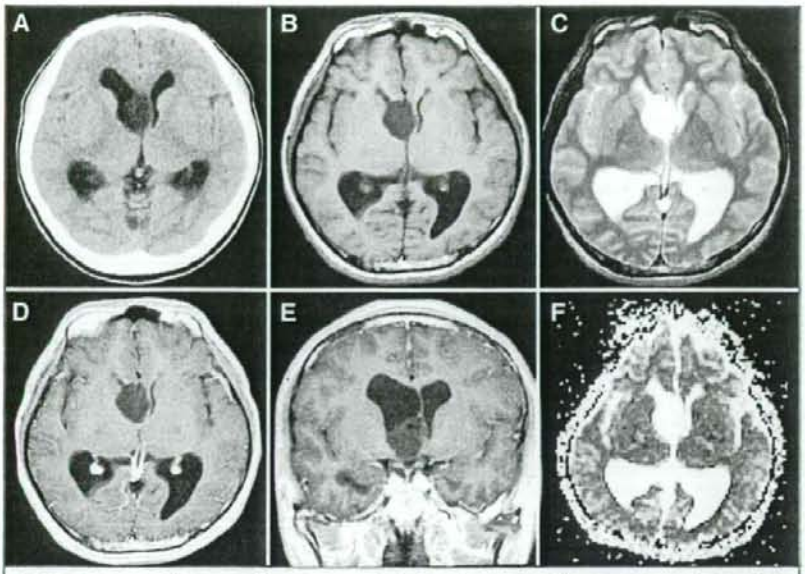

FIGURE 4. A, *plain CT scan revealing an intraventricular low-density mass adjacent to septum pellucidum.* B–F, *MRI scans before surgery. The intraventricular mass is hypointense on T1-weighted (B) and hyperintense on T2-weighted (C) MRI scans. Axial (D) and coronal (E) T1-weighted MRI with gadolinium showing nonenhanced mass occupying the anterior part of the third ventricle.* F, *the mass is hyperintense on axial section of apparent diffusion coefficient map image.*

reliably cured with surgical excision alone and that adjuvant therapy is unnecessary.

Because DNT-like neoplasms of the septum pellucidum are extremely rare and have only recently been described in the literature, we suspect that some previously reported intraventricular tumors, such as intraventricular oligodendroglioma, pilocytic astrocytoma, central neurocytoma, clear cell ependymoma, and subependymoma, were actually DNT-like neoplasms. From the viewpoint of treatment strategy, it is important to distinguish between DNT-like neoplasms and other low-grade infiltrating neoplasms, to avoid unnecessary adjuvant therapy (chemotherapy or radiotherapy). Histopathologically, DNT-like neoplasms of the septum pellucidum can be misdiagnosed as intraventricular oligodendroglioma, clear cell ependymoma, or central neurocytoma because of their similar histologic characteristics. However, the specific glioneuronal elements associated with DNT-like neoplasms are sufficiently distinctive to enable us to differentiate DNT-like neoplasms from oligodendroglioma, clear cell ependymoma, and central neurocytoma. Furthermore, electron microscopic analysis is helpful for differentiating DNT-like neoplasms from clear cell ependymomas, by detecting ependymal features (i.e., microvilli and cilia). In addition, the absence of intratumoral Rosenthal fibers and eosinophilic granular bodies in DNT-like neoplasms differentiates it from pilocytic astrocytoma. The presence of neurons within DNT-like neoplasms also differentiates them from both pilocytic astrocytoma and subependymoma.

DNT-like neoplasms also have distinctive MRI characteristics that can facilitate their diagnosis. The present DNT-like neoplasms and previously reported DNTs and DNT-like neoplasms are hypointense on T1-weighted MRI and hyperintense on T2-weighted MRI. Gadolinium injection results in no enhancement or minimal peripheral enhancement of these tumors. These are nonspecific features of these tumors. Interestingly, both of the present tumors had a high ADC. We previously reported that ADC is useful for differentiation of some human brain tumors, particularly DNT (17). In an analysis of MRI scans of 275 brain tumors, we found that the ADC of DNT (mean ± standard deviation, $2.546 \pm 0.135 \times 10^{-3}$ mm^2/s) was clearly higher than that of other World Health Organization Grade 1 and 2 gliomas, including pilocytic astrocytoma ($1.659 \pm 0.260 \times 10^{-3}$ mm^2/s), subependymoma (1.516×10^{-3} mm^2/s), ependymoma ($1.230 \pm 0.1119 \times 10^{-3}$ mm^2/s), and oligodendroglioma (1.455×10^{-3} mm^2/s). In addition, the ADC of DNTs was higher than that of any other glioneuronal tumor, including central neurocytoma ($0.946 \pm 0.342 \times 10^{-3}$ mm^2/s), with no overlapping of ADC values. The markedly high ADC of DNTs may be attributable to the presence of large extracellular spaces and their cellularity, which is much lower than that of other human brain tumors. These findings are consistent with the present cases, and we believe that preoperative ADC determination may facilitate differential diagnosis of DNT-like neoplasm of the septum pellucidum. It is possible that there might be a higher frequency of this disease than previously reported using the criteria of our study (histological and MRI findings), suggesting that there have been misdiagnosed tumors. Further studies, including examination of previous cases of tumors occurring in the septum pellucidum, are necessary to confirm the relationship between these findings and this rare category of neoplasms.

The molecular mechanisms underlying the pathogenesis of DNTs remain largely unknown. In the present report, DNT-like neoplasms occurred in the same location in the female patient and her nephew, with histopathological resemblance suggesting familial occurrence. Previously, Hasselblatt et al. (9) reported

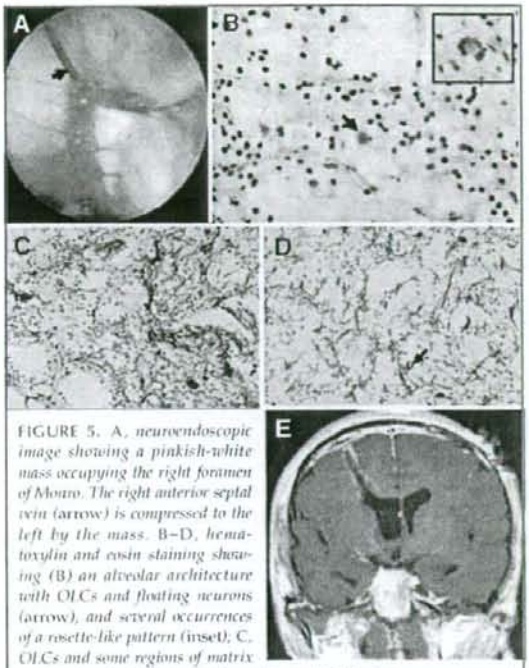

FIGURE 5. A, *neuroendoscopic image showing a pinkish-white mass occupying the right foramen of Monro. The right anterior septal vein (arrow) is compressed to the left by the mass.* B–D, *hematoxylin and eosin staining showing* (B) *an alveolar architecture with OLCs and floating neurons (arrow), and several occurrences of a rosette-like pattern (inset);* C, *OLCs and some regions of matrix positive for glial fibrillary acidic protein; and* D, *floating neurons (arrow) and other regions of matrix positive for neurofilament, whereas OLCs are negative.* (B, *original magnification,* ×400; C *and* D, ×200). E, *postoperative T1-weighted MRI showing no regrowth of residual tumor.*

occurrence of DNT in the same location (the left occipital cortex) in a father and daughter. They examined surgical specimens from both cases and performed comparative genomic hybridization (CGH) analysis but did not identify any chromosomal abnormalities common to both cases. They suggested that genomic hybridization can only detect large chromosome losses, whereas small deletions may be missed. In two other studies, researchers looked for genetic aberrations in DNT, including neurofibromatosis Type 1 gene deletion, *TP53* gene mutation, and loss of heterozygosity of chromosomes 1p and 19q, but did not find any such aberrations (5, 7). However, the familial occurrences in the present report and the report of Hasselblatt et al. strongly suggest that DNT and DNT-like neoplasms can be caused by a germline mutation; thus, it would be valuable to investigate the pathogenesis of these tumors. Recently, microarray-based CGH (array CGH) technology enabled high-resolution genome-wide deoxyribonucleic acid copy number analysis (15). Array CGH has emerged as a useful tool with which to detect and map genomic alterations, where putative oncogenes or tumor-suppressor genes may exist. Most recently, Idbaih et al. (10) analyzed nine patients with familial occurrence of glioma by array CGH and concluded that the technique is able to identify subtle differences that contain putative genes and are involved in the inheritance of familial gliomas. Therefore, the array CGH for patients with DNT-like neoplasm in this family may allow the identification of a gene locus for the occurrence of DNT-like neoplasms. Furthermore, the comparison of DNT-like neoplasms in this family and sporadic DNTs by array CGH may provide clues to the molecular pathogenesis of these tumors. However, more samples are required to obtain reliable data. Therefore, we will plan this as a future study in cases of DNT-like neoplasms developed in this family member and sporadic cases with DNTs.

CONCLUSIONS

The present report describes the first known familial occurrence of DNT-like neoplasm located in the septum pellucidum. The postoperative courses of the present cases were uneventful, and their residual tumors were stable on MRI, despite the lack of adjuvant therapy. The identification of this rare tumor in this rare location is important to avoid unnecessary adjuvant therapy, which is of no obvious benefit in such cases. The high ADC of this tumor on MRI and its histological findings of specific glioneuronal elements can facilitate the correct diagnosis of this tumor. The familial occurrences in the present report strongly suggest that DNT-like neoplasms of the septum pellucidum can be caused by a germline mutation. Further genetic study, including array CGH of affected patients in this family, could provide clues to its molecular pathogenesis.

REFERENCES

1. Baisden BL, Brat DJ, Melhem ER, Rosenblum MK, King AP, Burger PC: Dysembryoplastic neuroepithelial tumor-like neoplasm of the septum pellucidum: A lesion often misdiagnosed as glioma. Report of 10 cases. **Am J Surg Pathol** 25:494–499, 2001.
2. Cervera-Pierot P, Varlet P, Chodkiewicz JP, Daumas-Duport C: Dysembryoplastic neuroepithelial tumors located in the caudate nucleus area: Report of four cases. **Neurosurgery** 40:1065–1070, 1997.
3. Daumas-Duport C, Scheithauer BW, Chodkiewicz JP, Laws ER Jr, Vedrenne C: Dysembryoplastic neuroepithelial tumor: A surgically curable tumor of young patients with intractable partial seizures. Report of thirty-nine cases. **Neurosurgery** 23:545–556, 1988.
4. Daumas-Duport C, Varlet P, Bacha S, Beuvon F, Cervera-Pierot P, Chodkiewicz JP: Dysembryoplastic neuroepithelial tumors: Nonspecific histological forms. A study of 40 cases. **J Neurooncol** 41:267–280, 1999.
5. Fedi M, Anne Mitchell L, Kalnins RM, Gutmann DH, Perry A, Newton M, Brodtmann A, Berkovic SF: Glioneuronal tumours in neurofibromatosis type 1: MRI-pathological study. **J Clin Neurosci** 11:745–747, 2004.
6. Fujimoto K, Ohnishi H, Tsujimoto M, Hoshida T, Nakazato Y: Dysembryoplastic neuroepithelial tumor of the cerebellum and brainstem: Case report. **J Neurosurg** 93:487–489, 2000.
7. Fujisawa H, Marukawa K, Hasegawa M, Tohma Y, Hayashi Y, Uchiyama N, Tachibana O, Yamashita J: Genetic differences between neurocytoma and dysembryoplastic neuroepithelial tumor and oligodendroglial tumors. **J Neurosurg** 97:1350–1355, 2002.
8. Harter DH, Omeis I, Furman S, Braun A: Endoscopic resection of an intraventricular dysembryoplastic neuroepithelial tumor of the septum pellucidum. **Pediatr Neurosurg** 42:105–107, 2006.
9. Hasselblatt M, Kurlemann G, Rickert CH, Debus OM, Brentrup A, Schachenmayr W, Paulus W: Familial occurrence of dysembryoplastic neuroepithelial tumor. **Neurology** 62:1020–1021, 2004.

10. Idbaih A, Boisselier B, Sanson M, Crinière E, Liva S, Marie Y, Carpentier C, Paris S, Laigle-Donadey F, Mokhtari K, Kujas M, Hoang-Xuan K, Delattre O, Delattre JY: Tumor genomic profiling and TP53 germline mutation analysis of first-degree relative familial gliomas. **Cancer Genet Cytogenet** 176:121–126, 2007.
11. Kleihues P, Cavenee WK (eds): *Pathology and Genetics of Tumours of the Central Nervous System*. Lyon, IARC Press, 2000.
12. Kuchelmeister K, Demirel T, Schlörer E, Bergmann M, Gullotta F: Dysembryoplastic neuroepithelial tumour of the cerebellum. **Acta Neuropathol (Berl)** 89:385–390, 1995.
13. Kurtkaya-Yapicier O, Elmaci I, Boran B, Kiliç T, Sav A, Pamir MN: Dysembryoplastic neuroepithelial tumor of the midbrain tectum: A case report. **Brain Tumor Pathol** 19:97–100, 2002.
14. Leung SY, Gwi E, Ng HK, Fung CF, Yam KY: Dysembryoplastic neuroepithelial tumor: A tumor with small neuronal cells resembling oligodendroglioma. **Am J Surg Pathol** 18:604–614, 1994.
15. Shadeo A, Lam WL: Comprehensive copy number profiles of breast cancer cell model genomes. **Breast Cancer Res** 8:R9, 2006.
16. Whittle IR, Dow GR, Lammie GA, Wardlaw J: Dysembryoplastic neuroepithelial tumour with discrete bilateral multifocality: Further evidence for a germinal origin. **Br J Neurosurg** 13:508–511, 1999.
17. Yamasaki F, Kurisu K, Satoh K, Arita K, Sugiyama K, Ohtaki M, Takaba J, Tominaga A, Hanaya R, Yoshioka H, Hama S, Ito Y, Kajiwara Y, Yahara K, Saito T, Thohar MA: Apparent diffusion coefficient of human brain tumors at MR imaging. **Radiology** 235:985–991, 2005.
18. Yasha TC, Mohanty A, Radhesh S, Santosh V, Das S, Shankar SK: Infratentorial dysembryoplastic neuroepithelial tumor (DNT) associated with Arnold-Chiari malformation. **Clin Neuropathol** 17:305–310, 1998.

Acknowledgment

This study was supported in part by a Grant-in-Aid for Scientific Research from the Ministry of Education, Culture, Sports, Science and Technology of Japan (Grant no. 18591591).

COMMENTS

Saito et al. present a compelling case report about a very rare class of neoplasms. They claim that these are the first known occurrences of dysembryoplastic neuroepithelial tumor-like neoplasms located in the septum pellucidum in two related individuals. They demonstrate that two unique properties of these tumors, a high apparent diffusion coefficient and histological findings of "specific glioneuronal elements" may be distinguishing hallmarks of these neoplasms, setting them apart from other neoplasms of the central nervous system. This finding has important ramifications in that accurate identification of these neoplasms will avoid unnecessary use of adjuvant therapy associated with other central nervous system tumors as surgery alone appears to be an effective treatment strategy.

One clear limitation of the study, however, is the small sample size. To extrapolate these findings to a greater patient population, it would be necessary to see whether such observations hold true in similar patients. The rare frequency of this disease makes it challenging to examine such a large population in one study, and it is understandable that Saito et al. were limited in that context. However, with use of the criteria offered by this study, the frequency of this disease may be higher than previously reported, suggesting that some of these tumors may have been misdiagnosed. Regardless, additional patients need to be studied to confirm a more direct relationship between these findings and this rare category of neoplasm.

Saito et al. are eager to state that this is the first familial example of these tumors; however, they provide no hard evidence or discussion of the blood relationship of the patients in the study. Perhaps a genetic analysis or a discussion of how these patients were determined to be blood relatives is warranted. All in all, these findings provide very interesting observations and a framework for future researchers to pursue with more rigor and higher sample size.

Ahmed Mohyeldin
Neurobiologist

Alfredo Quiñones-Hinojosa
Baltimore, Maryland

In this well-written report, Saito et al. described two patients who presented with intraventricular/septum pellucidum dysembryoplastic neuroepithelial tumor-like tumors. The familial occurrence of this rare tumor led the authors to suggest a common germline mutation. The unusual location of this presentation, the septum pellucidum, is worth noting, as dysembryoplastic neuroepithelial tumors are typically located in cortical regions.

As a side note, I want to make a technical point. In both of these patients, Saito et al. selected the transcortical (transfrontal) trajectory to the frontal horn. In our practice, for these types of tumors with the size of the ventricles shown on the preoperative magnetic resonance imaging scans, we prefer the interhemispheric transcallosal approach. In our opinion, this is a less invasive trajectory compared with the transcortical one; the latter point is demonstrated in the postoperative coronal magnetic resonance imaging scan (*Fig. 5E* in the article) showing the residual zone of the trajectory itself. Saito et al. have not only reported this familial occurrence of a rare tumor but have also achieved good results in both of their patients.

Saleem I. Abdulrauf
St. Louis, Missouri

J Neurooncol (2007) 82:193–198
DOI 10.1007/s11060-006-9267-1

CLINICAL STUDIES—PATIENT STUDIES

Survivin subcellular localization in high-grade astrocytomas: simultaneous expression in both nucleus and cytoplasm is negative prognostic marker

Taiichi Saito · Muhamad Thohar Arifin · Seiji Hama · Yoshinori Kajiwara · Kazuhiko Sugiyama · Fumiyuki Yamasaki · Toshikazu Hidaka · Kazunori Arita · Kaoru Kurisu

Received: 25 July 2006 / Accepted: 11 September 2006 / Published online: 7 December 2006

Abstract
Objective Subcellularly localized(nuclear and/or cytoplasmic) survivin has various functions, and correlates with prognosis of malignant tumors. However, there have been no reports about the significance of subcellularly localized survivin in high-grade astrocytomas. The aim of the present study was to examine the relationship between prognosis and subcellular localization of survivin in high-grade astrocytoma.
Methods We immunohistochemically examined the pattern of subcellular localization of survivin expression (nuclear, cytoplasmic, or both) in 51 patients with high-grade astrocytoma (19 anaplastic astrocytomas; 32 glioblastomas). We statistically examined the relationship between survivin localization and prognosis, using multivariate analysis including other clinicopathological factors (age, sex, WHO grade, extent of resection, MIB-1 labeling index, and expression of p53 and epidermal growth factor receptor).
Results All specimens stained positive for survivin: localized in nucleus only (nuclear-positive group), 10 cases (20%); localized in cytoplasm only (cytoplasmic-positive group), 23 cases (45%); simultaneous expression in nucleus and cytoplasm (nuclear-cytoplasmic group), 19 cases (35%). There was no significant difference in prognosis between the nuclear-positive group and cytoplasmic-positive group ($P = 0.796$). However, the nuclear-cytoplasmic group had significantly shorter overall survival than the nuclear-positive group and the cytoplasmic-positive group ($P < 0.0001$).
Conclusions We found that simultaneous expression of survivin in both the nucleus and cytoplasm is an important prognostic factor for high-grade astrocytoma. The present findings indicate that subcellular localization of survivin expression is a reliable prognostic factor for patients with this tumor.

Keywords survivin · high-grade astrocytoma · subcellular localization · prognosis

Abbreviations

EGFR	epidermal growth factor receptor
AA	anaplastic astrocytoma
GBM	glioblastoma
ACNU	1-(4-amino-2-methyl-5-pyrimidinyl)methyl-3-(2-chloroethy)-3-nytrosoureal hydrochloride

Introduction

High-grade astrocytoma is the most frequent and malignant brain tumor. It is categorized into 2 types: anaplastic astrocytoma (AA; World Health Organization [WHO] Grade III); and glioblastoma (GBM; WHO Grade IV). Because it is difficult to surgically remove the entire tumor, patients are often treated with radio- and chemotherapy. Several reports indicate that radiotherapy slightly prolongs survival of patients

T. Saito (✉) · M. T. Arifin · S. Hama · Y. Kajiwara · K. Sugiyama · F. Yamasaki · T. Hidaka · K. Kurisu
Department of Neurosurgery, Graduate School of Biomedical Sciences, Hiroshima University, 1-2-3 Kasumi, Minami-ku, Hiroshima 734-8551, JAPAN
e-mail: taiichi@hiroshima-u.ac.jp

K. Arita
Department of Neurosurgery, Graduate School of Medical and Dental Sciences, Kagoshima University, Kagoshima, JAPAN

with high-grade astrocytomas [1,2]. In another study of patients with high-grade astrocytoma, the 1-year survival rate after combined radio- and chemotherapy was 46%, which was only slightly higher than the overall 1-year survival rate of 40% [3].

Survivin is a member of the inhibitor-of-apoptosis protein family, and it regulates apoptotic cell death and cellular proliferation. It is expressed at high levels in malignant tumor cells, and appears to play a role in tumorigenesis and prognosis of many malignant tumors [4-6]. We and others have demonstrated that expression of survivin mRNA or protein is a prognostic factor for gliomas [7–10]. Some researchers have argued that the effects of survivin on gliomas are stronger than those of certain other molecules, including epidermal growth factor receptor (EGFR), p53, bcl-2, and Ki-67 [8, 9]. Many recent studies indicate that functions of survivin (regulation of cell division or anti-apoptotic function) and its effects on tumorigenesis vary depending on its subcellular localization [11–15]. Therefore, determination of subcellular localization of survivin is necessary to estimate its effects on characteristics of malignant tumors. However, there are no previous reported studies of correlation between localization of survivin expression and prognosis in high-grade astrocytoma.

Therefore, in the present study of patients with high-grade astrocytomas, we immunohistochemically examined the pattern of subcellular localization of survivin expression in the tumor (nuclear, cytoplasmic, or both), and analyzed the relationship between survivin localization and prognosis. We also investigated the relationship between survivin localization and the molecules p53, EGFR and Ki-67, which are considered potential modulators of malignant progression and prognostic factors of high-grade astrocytomas.

Materials and methods

Clinical data and patient selection

Prior written informed consent was obtained from the patients and/or their guardians. We retrospectively studied the records of 51 patients (29 males and 22 females) with high-grade astrocytomas who were surgically treated at Hiroshima University Hospital between January 1994 and March 2004. All tumor samples were obtained during the initial operation. The patients ranged in age from 15 to 79 years (mean age [± standard deviation], 51.3 ± 19.6 years; median age, 56 years). Follow-up data of the patients were obtained from hospital records. To identify the prognostic factors of astrocytic tumors, we standardized the conditions that would affect prognosis. We excluded high-grade astrocytomas of the brain stem or cerebellum. We excluded pilocytic astrocytomas and diffuse astrocytomas, because they are classified as low-grade astrocytomas. We excluded other types of glioma, such as oligodendroglial tumors, ependymal tumors, and gangliogliomas, because they are pathologically distinct from astrocytic tumors. We excluded patients who did not receive radiation therapy, because craniotomy and adjuvant radiotherapy are standard treatments for high-grade astrocytoma. Patients with high-grade astrocytoma often also receive combined adjuvant chemotherapy; in Japan, this chemotherapy generally consists of treatment with 1-(4-amino-2-methyl-5-pyrimidinyl) methyl-3-(2-chloroethy)-3-nytrosoureal hydrochloride (ACNU). Because it is unclear whether chemotherapy significantly prolongs survival of patients with high-grade astrocytomas, we did not consider whether patients had received chemotherapy when selecting subjects for this study. Of the 51 patients enrolled in this study, 48 patients received ACNU-based chemotherapy.

Tissue specimens and immunohistochemical staining

All tumor specimens were obtained by surgical resection, and were fixed in 10% formalin before paraffin processing. Representative slides were stained with hematoxylin and eosin for standard histological diagnosis. Tumors were classified into histological subtypes by one of the authors (K.S.), according to WHO criteria. In the assays for the p53 alteration and expression of survivin, Ki-67 and EGFR, we used formalin-fixed, paraffin-embedded tumor samples. The primary antibodies used were a goat polyclonal antibody (Santa Cruz Biotech, CA, USA) at a 1:100 dilution for survivin, mouse monoclonal antibody (antibody MIB-1; Immunotech, Marseille, France) at a 1:50 dilution for Ki-67, a mouse monoclonal antibody (DAKO JAPAN, Kyoto, Japan) at a 1:100 dilution for mutant p53, and a mouse monoclonal antibody (Novocastra Laboratories Ltd., Newcastle, United Kingdom) at a 1:40 dilution for EGFR. Pathologic specimens (thickness, 4 μm) were mounted on gelatin-coated slides and deparaffinized by 15-min xylene treatment. To block endogenous peroxidase, the slides were immersed for 30 min in 3% hydrogen peroxidase in methanol. Each specimen was rinsed 3 times for a total of 15 min in phosphate-buffered saline, pH 7.5, with gentle stirring. They were then incubated overnight with the primary antibody at 4 °C. Next, the